The characterization of deep convective cloud albedo as a calibration target using MODIS reflectances

David R. Doelling[*a] , Gang Hong[b], Dan Morstad, Rajendra Bhatt[b], Arun Gopalan[b], Xiaoxiong Xiong[c],
[a]NASA Langley Research Center, 21 Langley Blvd MS 420, Hampton, VA 23681-2199 USA
[b]SSAI, One Enterprise Pkwy Ste 200, Hampton, VA 23666 USA
[a]NASA Goddard Space Flight Center, Lanham, MD 20706 USA

*d.r.doelling@larc.nasa.gov; phone 1.757.864-2155; http://www-pm.larc.nasa.gov

ABSTRACT

There are over 25 years of historical satellite data available to climate analysis. The historical satellite data needs to be well calibrated, especially in the visible, where there is no onboard calibration on operational satellites. The key to the vicarious calibration of historical satellites relies on invariant targets, such as the moon, Dome C, and deserts. Deep convective clouds (DCC) also show promise of being a stable invariant or predictable target viewable by all satellites, since they behave as solar diffusers. However DCC have not been well characterized for calibration. Ten years of well-calibrated MODIS is now available. DCC can easily be identified using IR thresholds, where the IR calibration can be traced to the onboard blackbodies. The natural variability of DCC albedo will be analyzed geographically and seasonally, especially difference of convection initiated over land or ocean. Functionality between particle size and ozone absorption with DCC albedo will be examined theoretically. Although DCC clouds are nearly Lambertian, the angular distribution of reflectances will be sampled and compared with theoretical models. Both Aqua and Terra MODIS DCC angular models were consistency consistency. The DCC method was able to identify two discontinuities in the Terra Collection 5 and validated the calibration of MODIS to within 0.1% per decade. Improvements to the DCC method need to take into account the functionality of 0.65µm DCC radiance with 11µm brightness temperature threshold and the DCC 0.65µm radiance difference over the tropical western pacific than over land afternoon generated DCC. Both of these cases cause a bias on order of 5%. These improvements should allow the first steps in using DCC as an absolute calibration target.

Keywords: Calibration, MODIS, Deep Convective Clouds

1. INTRODUCTION

In order to calibrate a 25-year historical record of un-calibrated geostationary and AVHRR satellite, absolute calibration targets. Currently desert, Dome C over Antarctica, and the moon are used as invariant targets, with occasionally congruent overpass flights of well-calibrated aircraft and satellite sensors such as MODIS. The advantage of deep convective cloud (DCC) is that they are found across the tropics and can calibrate all geostationary and AVHRR sensors. Most DCC are at the tropopause level and hence the effects of water vapor and tropospheric aerosol absorption are minimized. Also the DCC technique (DCCT) does not rely on navigation to find its target, but relies on co-registration of the visible and IR pixels. The DCCT relies on calibrated IR brightness temperatures (BT) to identify the coldest convective cells. Most historical satellites have onboard blackbodies making this DCCT possible. The DCCT uses convective clouds as bright earth targets that have a predictable albedo, which are nearly Lambertian for small view and sun angles. These are small angular dependencies can be modeled or derive using observations during a time period where the instrument calibration was considered stable. Observational derived angular models can account for the absorption lines inside the bandwidth of the visible channel.

To use the DCCT for absolute calibration, the geographical, diurnally and seasonal variations of the DCC cloud microphysics need to be characterized. The absolute calibration of geostationary satellites relies on geographical uniform DCC albedos to ensure calibration consistency across satellite boundaries. The Terra and Aqua time difference allows evaluation of DCC albedos diurnally. There are now 10 and years of Terra and Aqua available to study seasonal effects. This study characterizes Terra and Aqua MODIS DCC radiances geographically as well as a function of

viewing and solar geometry. Comparing with the MODIS calibration, which uses solar diffusers, will validate the DCCT robustness.

2. DEEP CONVECTIVE CLOUD CALIBRATION METHODOLOGY

The DCCT was first demonstrated by Hu et. al (2004)[6] in order to verify that the observed fluxes on the Clouds and the Earth's Radiant Energy System (CERES) instrument onboard the Tropical Rainfall Measuring Mission (TRMM) satellite were well calibrated for stability. He identified the DCC footprints 20km by using a simple mean Visible Infrared Scanner (VIRS)11μm brightness temperature threshold. He plotted the monthly global ensemble of footprint SW fluxes as probability distribution functions (PDF) and showed that they had the same shapes over 8 months and were on top of each other indicating no change in the stability of the CERES instrument. The CERES SW radiances, which are a function of view and azimuth angle were first converted to flux using the CERES Bidirectional Reflectance Function (BDRF) or Angular Distribution Model (ADM)[3] designed for the brightest ice clouds. This validated that DCC had predictable albedos, since they are nearly Lambertian at low sun angles, at the TOA with very small gaseous absorption in the near infrared. The record of TRMM fluxes was short as to not have any impact from long-term variations of stratospheric ozone and aerosol from volcanoes. Doelling et al. (2004) with limited success implemented the same DCCT to calibrate the AVHRR visible radiances (0.65μm and 0.86μm) onboard NOAA-16 and 17. In this case the CERES broadband ADM was also used to convert the AVHRR narrowband radiances into overhead sun radiances. The DCCT calibration method was verified with using ground track intersect ray matched radiance technique to transfer the MODIS calibration to AVHRR of similar bands. Accuracy of the AVHRR navigation was not needed, only good co-registration of the visible and IR channels. Minnis et al. 2008[5] used DCCT to verify the calibration of the VIRS and MODIS instruments. It was shown that for VIRS Version 5a had stable calibration coefficients, however Version 6 calibration was found to have a definite drift over time. It was also shown a one time change in November 2003 the DCCT identified a 1.2% jump in the Terra-MODIS radiances.

The DCCT employed in this study uses the same thresholds as used in Minnis et al. 2008. The tropical domain is restricted to be within 30°N and 30°S. Every MODIS granule that falls within the domain was used. Every other month was considered to reduce processing time. The Terra-MODIS data was processed from March 2000 to July 2010 and the Aqua-MODIS from 2003 and from November 2005 to July 2010. The actual Aqua-MODIS record begins in July 2002 to the present, however for this study 2002 and January to October 2005 was unavailable at the Langley archive. This usually entails four 5-minute granules along the ground track. The MODIS pixels have a nominal resolution of 1-km at nadir, utilized only every other pixel and line. All MODIS pixels that had a band 31 (11μm) brightness temperature < 205°K were considered. The pixels viewing geometry was restricted to solar zenith angle (SZA) < 40° the viewing zenith angle (VZA) < 40° and the relative azimuth angle (RZA) was between 10° to 170°. To further increase the confidence that DCC were identified, the 8 surrounding pixel band 1 (0.65μm) radiance standard deviations were restricted to 3% and the 11μm sigma < 1°K. The 0.65μm radiances were converted to overhead sun by using the CERES ADM and directional model (albedo as a function of solar zenith angle) for ice clouds with optical depths greater than 50. Collection 5 MODIS radiances were used. The intention later would be to use the MODIS instrument team Collection 6 from 5 calibration adjustment factors to convert the radiances to Collection 6 quality.

3. DCCT BDRF VALIDATION

Two methods were used to track the DCC radiances over time. All of the tropical DCC identified 0.65μm nadir radiances for the month, were plotted as a probability distribution function (PDF). The nadir radiance with the greatest frequency is the mode method, whereas the average of all radiances is known as the mean method. To ensure that the CERES ADM accurately predicted the DCC angular radiance variability, DCC PDFs can be stratified as a function of angle. Figure 1c shows the PDF of the 0.65μm Terra-MODIS DCC nadir radiances stratified by VZA for the month of November 2000. This month was displayed, since the month had the greatest number of DCC pixels over the entire record. The red line shows all VZA < 40° (labeled inaccurately) and then in 8° VZA increments. The number of DCC pixels are given in column 2 in the upper left statistics and are usually on order of ~ 0.5M to 1M per month. Notice that all of the PDF shapes are very similar with mean (column 3) and mode (column 4) method giving nearly identical DCC radiances, which are within 1.5%. Similarly, Figure 1d shows the VZA PDFs for Aqua-MODIS during May 2004. Note that the Aqua-MODIS DCC radiances are slightly greater than Terra-MODIS inferring that the Aqua-MODIS absolute calibration is slightly higher. The MODIS team claims an absolute calibration uncertainty of 2%. However the DCC Aqua-MODIS radiances stratified by VZA are also within 1.5%. Figure 2e and 2f show the DCC radiance PDF

stratification according to azimuth angle. Again the DCC radiances based on either the mode or mean methodology stratified by RZA are within 1.5%. The SZA stratification revealed similar results but not shown. Also the SZA for both Terra and Aqua MODIS were limited between 20° to 40° in the tropical domain. This validates that the CERES ADM is capturing most of the DCC angular variation. Also the DCC radiance PDFs stratified by sigma of the 11μm brightness temperature and 0.65μm radiances were nearly identical. The PDFs for sigma greater than 1°K and 3%, respectively, produced a more uniform frequency and therefore not used in analysis (not shown).

However there is a functionality of DCC nadir radiances based on 11μm brightness temperature (BT). Figure 1a and 1b show the DCC radiance PDF as a function of BT. The colder the BT the greater the DCC nadir radiance. There is a ~3% increase in the DCC nadir radiance between BT stratifications. Also the PDF has a stronger peak feature. This is preferable for the DCCT and indicates that only the brightest clouds were identified and reducing the uncertainty of the technique. However reducing the BT threshold dramatically reduces the number of identified DCC by ~ 15% and if the BT threshold was restricted < 195°K some months would not have enough DCC pixels for a smooth PDF and increasing the uncertainty of the method for stability. To improve the DCCT this functionality can be modeled and eliminating possible biases resulting from the non-uniform monthly PDF due to variations deep of convective microphysics.

4. DCCT CALIBRATION OF TERRA AND AQUA MODIS

Now that the DCCT produces uniform monthly PDFs using the CERES ADM with the given thresholds to identify DCC clouds, the monthly mode and mean method DCC nadir radiances are plotted over time, as a function of day since launch in Figure 2a for Terra-MODIS. The accompanying mean and mode method linear regressions are also shown. There is a definite downward trend in the DCC nadir radiances. However there are two definite discontinuities in the timeline. The first one is at November 2003 and was identified by Minnis et al 2008 and if the gain of the MODIS radiances after November 2003 was increased by 1.011 removed the bias at the first discontinuity. The second discontinuity is at June 2009 and if a gain of 1.022 is applied after June 2009 has successfully removed the bias. The second discontinuity was a result of the re-evaluation of the solar diffuser degradation for various channels based on assumption that the 0.91μm solar diffuser channel does not degrade. Figure 2c shows the normalized monthly DCC nadir radiance to the mean of the 10-year record. The mean 10-year DCC nadir radiance is given in the last line of the linear regression statistics at the bottom of the plot for both the mean and the mode methods. The above-mentioned gain adjustments were applied to the Terra-MODIS normalized radiances. The slope of the regression, shown in day^{-1}, is within .1% over the decade for both mean and mode methods. The standard error of the mode method is half of that of the mean method. The mode method is robust for most months when given enough sampling to produce a well-defined peak. The mode method is independent of the tails of the PDF, whereas the mean method is affected. Much effort using thresholds of various parameters were used to limit the tails, but were unsuccessful. The dark side of the tail is optically thin cirrus in the visible that is optically thick in the IR. More than likely it is cirrus blow off from deep convection that have a very uniform temperature at the TOA but the cloud thickness is decreasing. The tropopause in the tropics is very isothermal and is being modified by the deep convection.

Figure 2b and 2d show the corresponding plots for Aqua-MODIS. For Aqua no discontinuities were found and no adjustments were performed. In this case the mean and mode methods provided a difference in the slope of the linear regression, however well within the standard errors of the fit, showing no statistical significance in the trend. The mode and mean method shows the trend is less than 0.7% and 0.1% over the decade, which confirms that stability of the MODIS sensor, which uses the sun as its calibration source. Again the standard error of the mode is half of the mean method for Aqua-MODIS. The mean DCCT method nadir radiance is 4.1% less than the mode method for Terra and 4.6% for Aqua. This implies that the DCC pixels level radiance dependencies are consistent between Terra and Aqua sampling times. The Terra and Aqua are in a 10:30AM and 1:30PM local time sun-synchronous orbits and the measurements are symmetric about solar noon, thus providing the similar sampling. The mean Aqua-MODIS nadir DCC radiance from the mode method is 1.5% and 1.0% greater than Terra-MODIS for the mode and mean DCCT methods, respectively, consistent with previous results in this study.

5. DCCT ANALYSIS GEOGRAPHICALLY AND SEASONALLY

In order to further evaluate the consistency between Terra and Aqua derived DCC radiances, and more importantly geographical and diurnal effects on the DCC microphysical characteristics, spatial and temporal analysis is

performed. If the DCC predicted radiances are uniform across the earth than DCCT could be used as an absolute invariant calibration target. For example if geostationary satellites were absolutely calibrated using DCCT then the calibration across satellite boundaries would be seamless. Also if land afternoon convection and ocean derived DCC radiances microphysics were uniform possibly the geostationary calibration can be evaluated diurnally and over some geostationary domains both land and ocean geo-types can used to increase DCC sampling. For this study the diurnal DCC difference is limited and is evaluated using Terra and Aqua differences separated by 3 hours at the equator. Terra and Aqua time differences centered at noon increases in the southerly direction and decreases in the northerly direction. However since polar orbiting circumnavigate the globe daily with a small spatial sampling gap between orbits at the equator limited by the 14 orbits a day at 70° VZA and much greater sampling gap for 40° VZA. However the polar orbit repeats every 16 days and the ground track is nearly overhead every 8 days for any given site, so that over the course of the month uniform sampling across the tropical domain is achieved.

DCC clouds are normally observed in the Inter-Tropical Convergence Zone (ITCZ) over oceans, which follow the sun during the course of the year. Over land DCC peak in the late afternoon and also migrate over the year. DCC are not found over maritime subsidence zones where stratus clouds dominate or over land in desert regions. To quantify the spatial frequency of the DCCT of this study the tropical domain was gridded into 5° latitude by 5° longitude regions. Figure 3a shows the Terra-MODIS spatial frequency of DCC for January. All of the Januaries during the Terra record were summed. The total pixel count for some regions over the Tropical Western Pacific (TWP) is over 100000. The Indian and west Pacific domains having the greatest frequency of DCC sampled at 10:30AM. The land convection is quite limited over the Amazon and Congo River basins. The ITCZ is easily identified over the east Pacific and Atlantic oceans. Figure 3b displays the July frequency. Most of the southern hemisphere DCC has shifted to the northern hemisphere. Increase convection is apparent over Central America and India during its monsoon season. Again land convection is quite limited in the morning. Figure 3c shows the 10-year mean of the frequency of Terra-MODIS identified DCC. The TWP and East Indian Ocean regions overwhelmingly have the greatest frequency of DCC. Other prime locations for DCCT calibration are over the east Atlantic, oceans surrounding Central America and Southern Pacific Convergence Zone. Even over the year land morning convection frequency is secondary to oceans. However most geostationary satellites will benefit from DCCT calibration. To access the consistency of the DCCT nadir radiance, the average of all the radiances in region is taken and plotted. Only regions with more than 20000 pixels are considered, since the Puffs give spurious results when under sampled. Figure 3d quickly identifies the difference between TWP and land DCC radiances. These differences are on order of 5%. If the DCC frequency over a given region does not change in time than this effect is minimized. However to absolute calibrate geostationary visible instruments will need modification of the DCCT method. Some possible explanations for this feature is that the convection over the TWP rises more slowly since there is a steady cycle of convection, thereby creating a more stable atmospheric profile, than over land regions where diurnal heating creates an unstable atmosphere increasing the vertical motion thereby inducing microphysical properties different than over the TWP.

Figure 4a shows the January distribution for DCC for Aqua. The complete Aqua record for this study entails 53 months, whereas the Terra record is 123 months. Figures 4a and 4b can be compared with Figures 3a and 3b after normalizing the Aqua frequency by 123/53. Figure 5c has been frequency has been normalized with Terra. It is obvious from Figure 4a and 4b and 4c that the land afternoon convection increases the DCC frequency for Aqua, especially over the Amazon and Congo basins. Again the TWP has the greatest frequency of DCC. Figure 4d is very similar to Figure 3d, implying that the consistency of DCC diurnally over oceans. Also over land the DCC radiances are similar, although the convection times are different, indicating the microphysics over land are consistent diurnally. Only regions with DCC frequencies greater than 20000 are used, however there are some regional outliers of dark DCC radiances. As with Terra most geostationary satellites can benefit from DCCT calibration, however the mean DCC nadir radiance is 5% darker over the TWP. Also the frequency of DCC increases from morning to afternoon.

6. DCCT TERRA/AQUA BDRF CONSISTENCY

Another consistency check between Terra and Aqua DCC radiances would be to stratify them angularly to note any changes in the BDRF that may be a factor due to diurnal changes of the cloud microphysics. Also another way to improve DCCT methodology is to use BDRF specifically suited for the spectral response of the visible channel. Even though DCC are at the TOA there is still some absorption due to ozone and oxygen bands. If the BDRFs are derived from observations during a time period where the calibration is not known to have changed than the BDRF can be used for the lifetime of the satellite instrument. Since the CERES ADMs were derived from broadband spectrum and based on 20km footprints some differences between CERES ADM and one derived from MODIS are expected. The MODIS

0.65μm-bandwidth is very narrow and incorporates an ozone absorption band. Figure 5a and 5b shows the angular frequency for the 10° SZA bin centered at 25° for DCC for Terra during November 200 and Aqua during May 2004, respectively. It is remarkable the angular DCC sampling is very similar. Again as stated previously the Terra and Aqua local equator crossing times at the equator are symmetric about noon. Figure 5 is using the same population as Figure 1. As with Figure 1 Aqua had less overall sampling for the month but the same distribution evident. Figure 5c and 5d shows the mean MODIS reflectance, derived by the mean method. Note the VZA dependence on the reflectances similar to the radiative transfer model results in Figure 1. Again the Aqua DCCT reflectances are greater than the Terra reflectances for most angular bins, but still revealing same VZA dependency as Terra. Figure 5e and 5f show the normalized reflectance or BDRF for the 25° SZA bin, thereby taking out the Terra and Aqua MODIS calibration difference. The only difference between Terra and Aqua would be in the forward scattering direction, where the relative azimuth angle is near 0°. The Aqua seems to be more Lambertian in the forward scatter. The average albedo for Terra-MODIS is 0.93 and Aqua-MODIS is 0.94 again showing a 1% difference in calibration. Another check would be the angular bin variability. Figure 5g and 5h indicate the standard deviation of all DCCT nadir reflectances were in between 0.7 to 0.1 for most bins, which are well sampled. The relative azimuth angle bins near 90° show inconsistencies, however they are not well sampled. The angular variations between Terra and Aqua DCC nadir reflectances are very consistent.

7. CONCLUSIONS

In conclusion, the DCCT method outlined in this study is sufficient to calibrate the Terra and Aqua-MODIS DCC nadir radiances. The CERES ADM predicted DCC reflectances were used to convert or normalize the angular radiance to nadir radiance. The CERES ADM showed no dependencies with respect to SZA, VZA, and RAA, however improvements in reducing the angular uncertainty can be achieved by using ADM specifically derived from observations MODIS radiances. The Terra and Aqua derived ADMs were similar in nature. The DCCT method observed two discontinuities in November 2003 and June 2009 in the Terra Collection 5 radiances, which should be corrected for in the Collection 6 version. The Aqua DCC radiances were consistent over time. The MODIS instrument uses the sun as its calibration source as does the DCCT method, which uses DCC also as solar diffusers. After taking adjusting for discontinuities the Terra showed stability within 0.1% over the decade and the mean DCCT method of Aqua gave similar stability. However further improvement in the DCCT method outlined in this study can be achieved by taking into account the increase in DCC visible radiance with decreasing 11μm BT. Also the DCC visible radiance is 5% darker over the TWP compared with DCC created by land afternoon convection. These two improvements are needed to convert the DCCT methodology into an absolute calibration method. After these improvements the DCCT can be used to absolute calibrate geostationary seamlessly across satellite boundaries, since most geostationary satellites have sufficient DCC sampling to use the DCCT method.

REFERENCES

1. Doelling, D. R., L. Nguyen, and P. Minnis, On the use of deep convective clouds to calibrate AVHRR data. *SPIE49_5542-30*, *Proc. SPIE 49th Ann. Mtg., Earth Observing Systems IX Conf., Denver, CO, August 2-6.* 2004
2. Hu, Y**.,** B. Wielicki, P. Yang, P. Stackhouse, B. Lin, and D. Young, Application of deep convective cloud albedo observations to satellite-based study of terrestrial atmosphere: monitoring stability of space-borne measurements and assessing absorption anomaly. Accepted, *IEEE Trans*. *Geosci. Remote Sensing*, 2004.
3. Loeb, N. G., N. Manalo-Smith, S. Kato, W. F. Miller, S. K. Gupta, P. Minnis, and B. A. Wielicki, Angular distribution models for top-of-atmosphere radiative flux estimation from the Clouds and the Earth's Radiant Energy System instrument on the Tropical Rainfall Measuring Mission satellite. Part. 1: Methodology. *J. Appl. Meteorol.*, **42**, 240-265, 2003.
4. Minnis, P., L. Nguyen, D. R. Doelling, D. F. Young, W. F. Miller, Rapid calibration of operational and research meteorological satellite imagers, Part I: Use of the TRMM VIRS or ERS-2 ATSR-2 as a reference. *J. Atmos. Ocean. Technol.* **19**, 1233-1249, 2002.
5. Minnis, P., D. R. Doelling, L. Nguyen, Walter F. Miller, Venkatesan Chakrapani, Assessment of the Visible Channel Calibrations of the VIRS on TRMM and MODIS on Aqua and Terra *J. Atmos. Ocean. Technol.* **25**, 385-400, 2008.

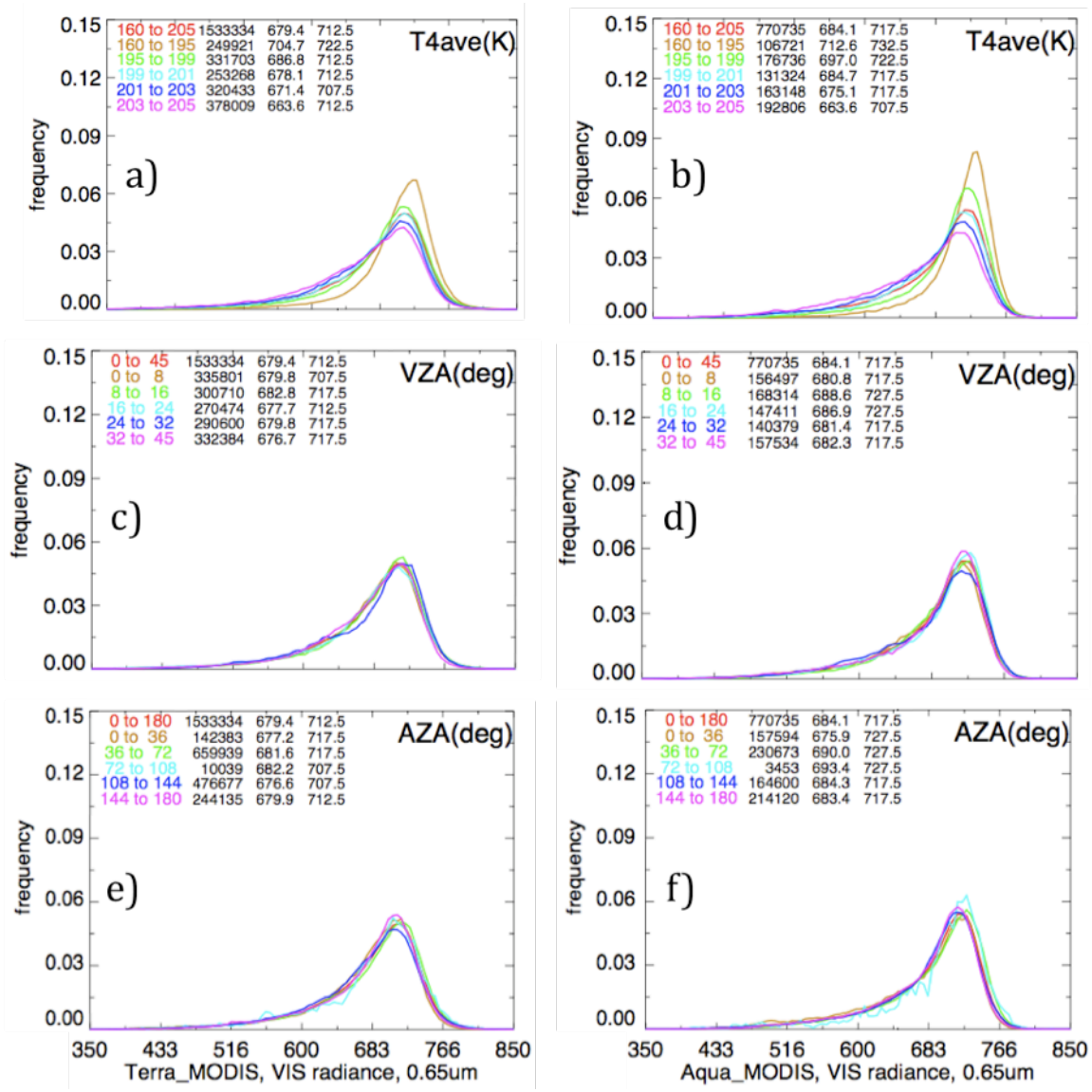

Figure 1: a) November 2000 probability distribution function of Terra-MODIS band 1 (0.65µm) deep convective reflective radiances ($Wm^{-2}sr^{-1}\mu m^{-1}$) over the tropical domain stratified by Terra-MODIS band 31 (11µm) brightness temperature ranges as given in the first column of the upper left corner of the plot. The second column indicates the number of deep convective identified pixels for that range. The third and fourth columns are the deep convective reflective radiances ($Wm^{-2}sr^{-1}\mu m^{-1}$) for the mean and mode methods respectively. The associated lines on the plot are color-coded based on the temperature ranges of the first column. c) Same as a) except that view zenith angle ranges are shown. e) Same as a) except that relative azimuth angle ranges are shown. All plots in the right column are for Aqua-MODIS for the month of May 2004 with the same associated parameters for each row as Terra-MODIS.

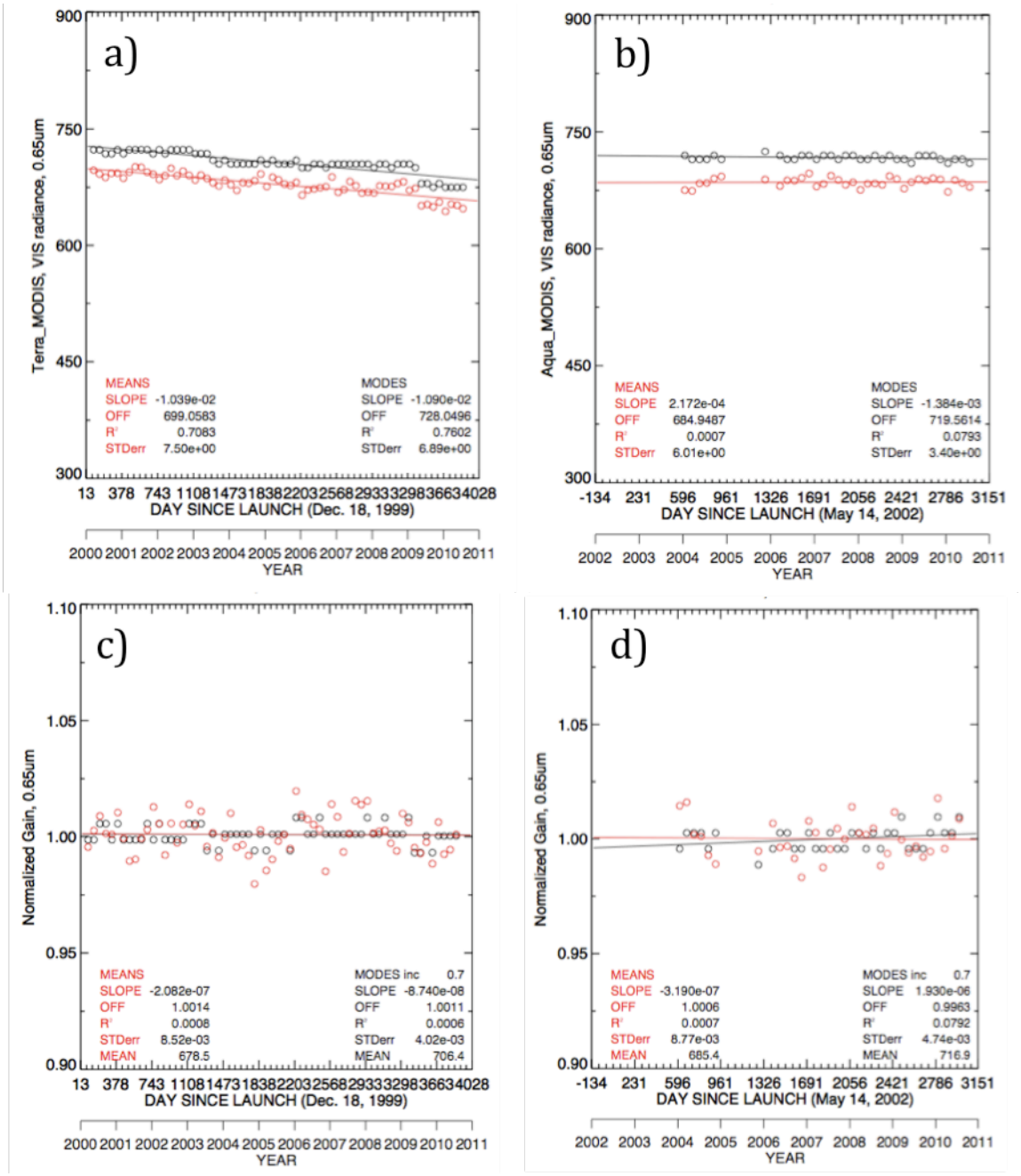

Figure 2: a) Terra-MODIS band 1 (0.65µm) bi-monthly variation of deep convective reflective radiances ($Wm^{-2}sr^{-1}\mu m^{-1}$) (open circles) plotted with linear regression fits (lines), for mode (in black) and mean (in red) methods. Linear regression statistics based on Terra day since launch are given in the lower left and lower right corners for the mean and mode method respectively. b) Same as a) except for Aqua-MODIS. c) Same as a) except that the normalized gain is plotted. d) Same as c) except for Aqua-MODIS

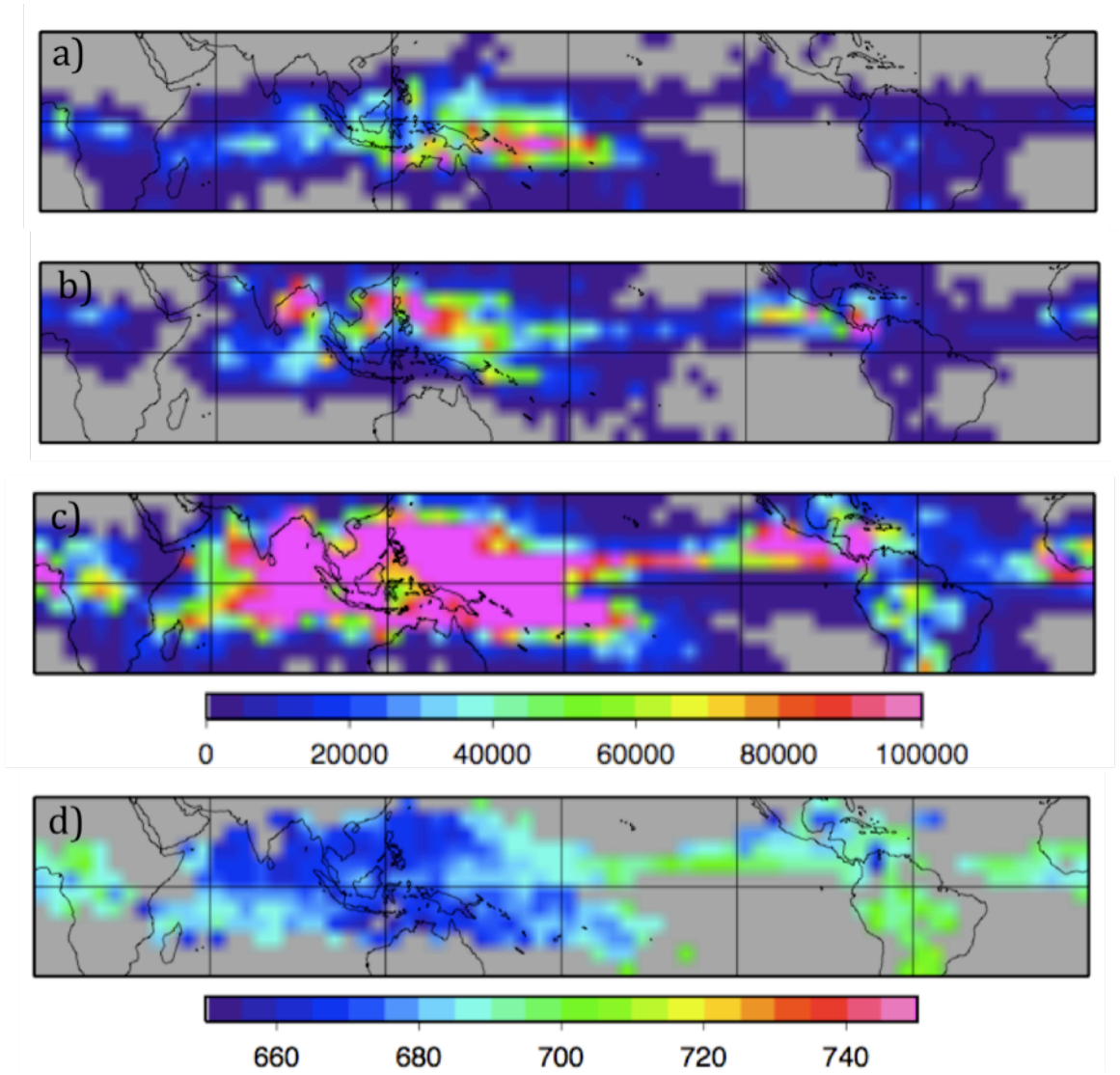

Figure 3: a) Terra-MODIS band 1 (0.65μm) 10 year sum of January deep convective cloud identified pixels (2 km pixel resolution) over the tropical domain based on a 5° by 5° latitude by longitude grid. b) Same as a) except for an 11 year sum of July pixels. c) Same as a) except during March 2000 to July 2010 bi-monthly sum of deep convective cloud identified pixels. The color-bar under c) is valid for a) and b) Note that many regions had more than 100000 deep convective pixels. d) The Terra-MODIS band 1 (0.65μm) mean of bi-monthly deep convective reflective radiances ($Wm^{-2}sr^{-1}\mu m^{-1}$) during March 2000 to July 2010 over the tropical domain based on a 5° by 5° latitude by longitude grid.

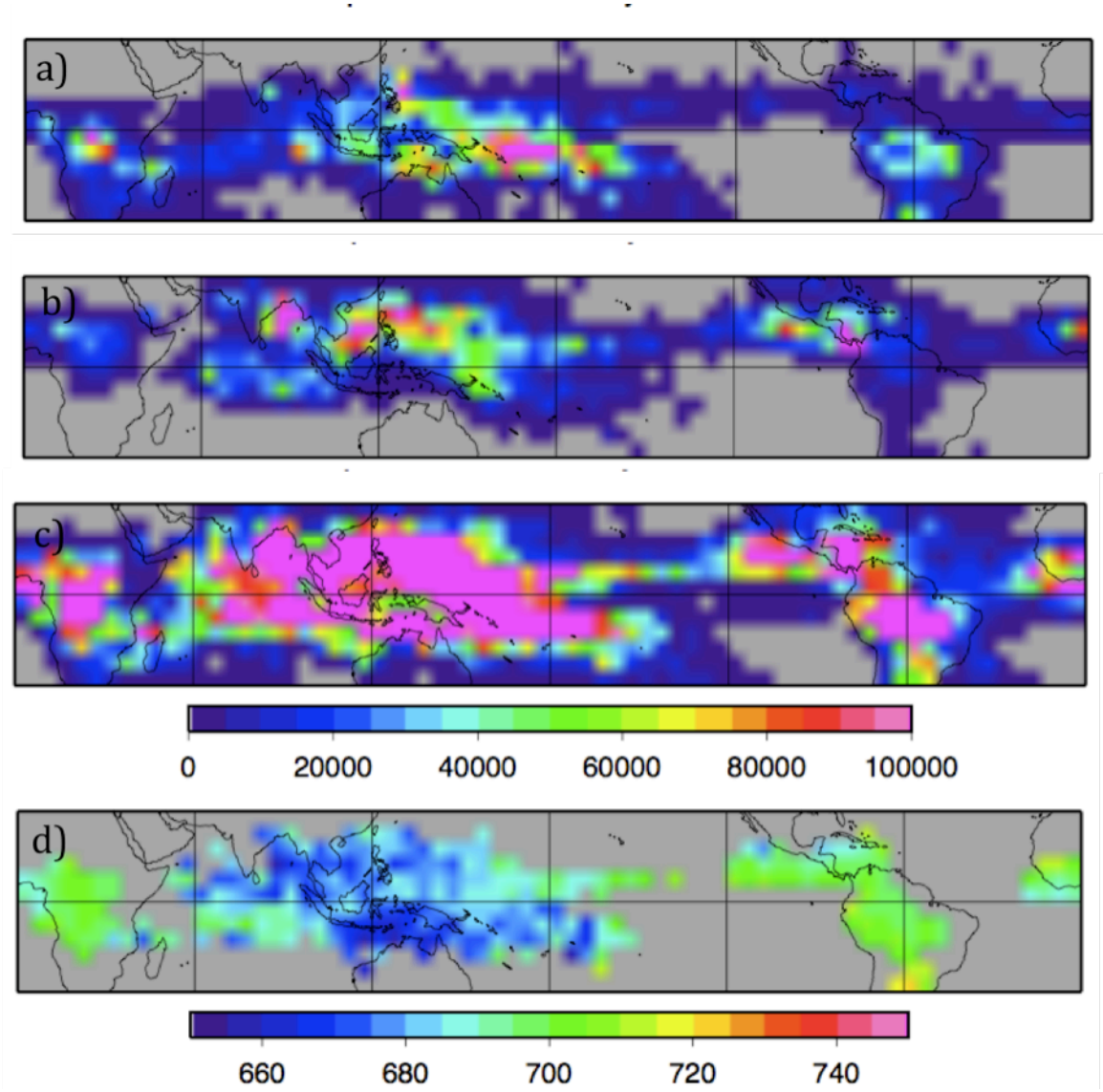

Figure 4: Same as Figure 3 except for Aqua-MODIS

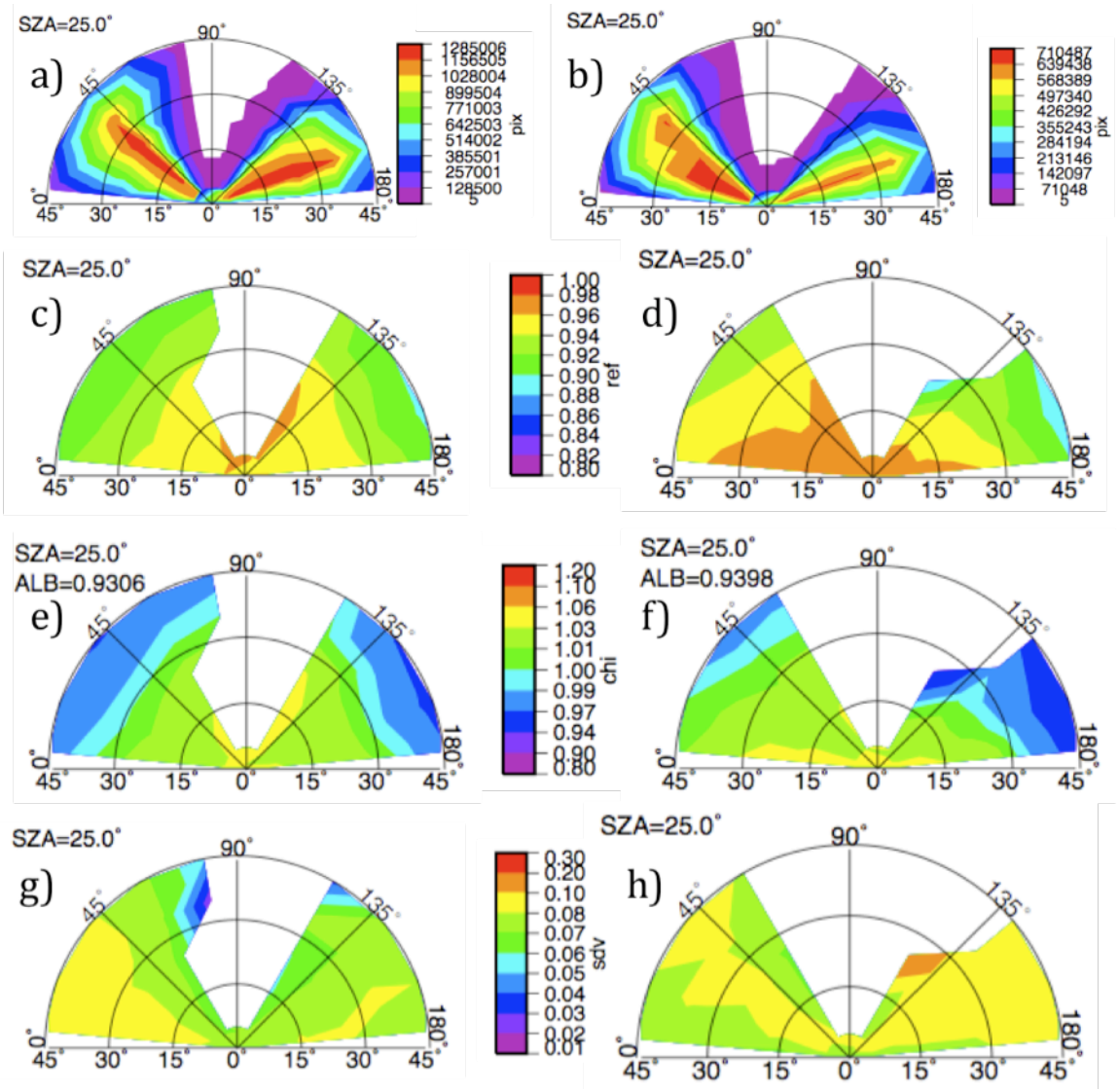

Figure 5: a) The bidirectional distribution of the number of deep convective identified pixels for Terra-MODIS band 1 (0.65μm) during November 2000 for a 10° solar zenith angle bin centered at 25°. The view angles are shown on the x-axis and the azimuth angle is shown radially, each with 10° bins. The associated color-bar legend is shown to the right of the plot. c) Same as a) except for deep convective reflectances. The color-bar is centered on the row. e) Same as a) except for BDRF of the reflectances. The mean albedo is given to the left of the plot. g) Same as a) except that the standard deviation of the reflectance is given. All plots in the right column are for Aqua-MODIS for the month of May 2004 with the same associated parameters for each row as Terra-MODIS.